Pebax® Supported Membranes for Post-combustion CO_2 Capture

Nanostructured Materials for Nanotechnological Application, INA, University of Zaragoza, Spain

Erasmus Mundus Masters in Membrane Engineering for a Sustainable World (EM3E-4SW)

Md Rafiul Hasan

Supervised by : Professor Joaquín Coronas

Dr. Magdalena Malankowska

www.em3e-4sw.eu

"The EM3E4SW Master is an Education Programme supported by the European Commission, the European Membrane Society (EMS), the European Membrane House (EMH), and a large international network of industrial companies, research centres and universities".

And

"The EM3E4SW education programme has been funded with support from the European Commission. This publication reflects the views only of the author, and the Commission cannot be held responsible for any use which may be made of the information contained therein".

Contents

List of Figures

List of Tables

Abstract:

Mixed matrix membranes (MMMs) with metal organic framework (MOF) as fillers is one of the growing fields of research for post combustion CO_2/N_2 separation. Pebax® MH 1657 polymer matrix and MOF ZIF-94 filler are the interested components for this research. Synthesized ZIF-94 particles were found polydisperse having average particle size of 175 ± 68 nm. Afterword, fillers were well dispersed in polymeric matrix which was confirmed by scanning electron microscopy imaging. Incorporation of ZIF-94 significantly improved performance of bare Pebax® membrane where maximum selectivity obtained was 43.5 (CO_2/N_2) for MMMs having 10 wt.% ZIF-94 loading in 9 wt.% of the polymer matrix which satisfies the corresponding upper bound plot. Reproduction of the results are under investigation which require more attempts. Here, the final report of result output is the average of recent and previous results which is selectivity of 29 and permeance of 170 Barrer.

Keywords: Gas separation, Mixed matrix membrane, Metal organic framework, ZIF-94, Pebax® MH 1657

1. Introduction

According to the International Energy Agency (IEA), fossil fuels are the primary energy source in anthropogenic activities. It is the major cause of CO_2 emission to the environment with 6% increment every year.[1] In general, post-combustion flue gas from coal-fired power plant contains 70-75% N_2, 10-15% CO_2, 8-10% H_2O, 3-4% O_2, with trace levels of SOx, NOx, and other compounds.[2] In recent years, National Oceanic and Environmental Administrative (NOEA) has reported that, concerning level of CO_2 accumulation in the atmosphere is becoming unavoidable problem in the 21st century. This gathering is considered as the key reason of global warming, causing unpredictable changes such as heat stress, increasing severity of tropical storms, acid rains, rising sea levels, and the melting of glaciers, snowpack and sea ice, etc. throughout the entire planet.[1] Additionally, IEA has forecasted an increasing tendency of energy demand around the globalized world, that is 57 % (from 2004-2030),[3] and an extensive release of greenhouse gases will continue if no precaution is taken either for searching of green energy sources or filtering post-combustion gases. Although few alternative energy sources are available, such technology is not mature enough to scale-up for industrial application which require a long-term goal. Hence, a treatment of flue gas for capturing CO_2 is a straightforward solution to avoid such challenging

concerns; this phenomenon is called carbon capture and storage (CCS). Around 95% of coal fired and 40% of gas fired power plants should be introduced with CCS system in order to limit the global temperature rise below 2 °C (which is predicted from Paris conference in 2015).[4] There are several possible technologies for CCS either based on solvents (absorption), solid adsorbents (adsorption), cryogenic process or membrane-based process which are summarized in Figure 1.[5,6]

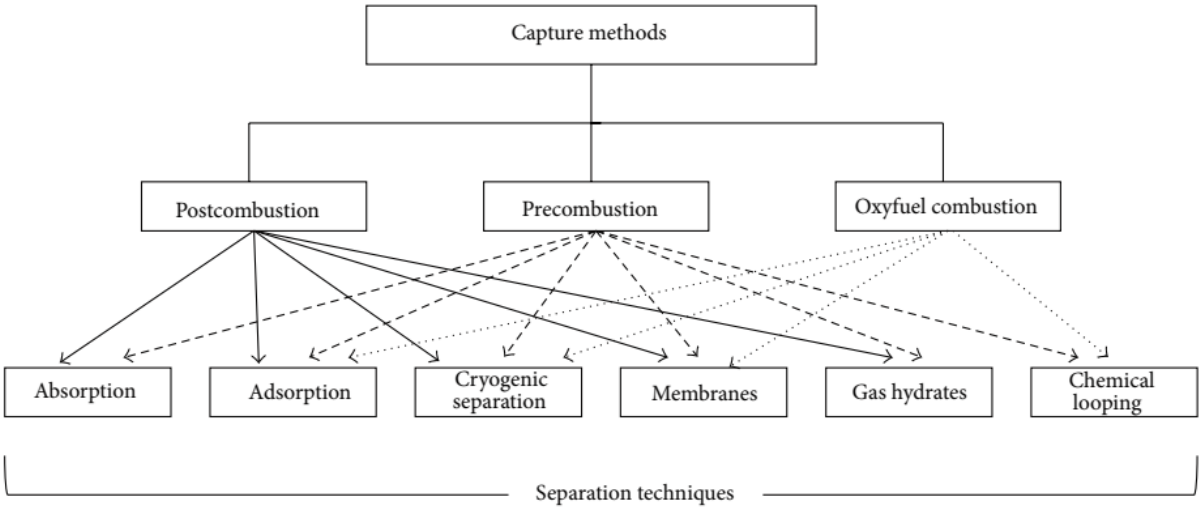

Figure 1:Different CCS based separation techniques. Taken from [6]

In general, CO_2 capture based on chemical solvent treatment is more efficient than physical adsorption (90% share of CCS in the market is amine based absorption), even blended composition provide better capture throughput than a single solvent.[1,7] The "conventional solvents", well-known for present high CO_2 sorption capacity, were commercialized in 1930s. They can be divided into chemical and physical strippers. The physical strippers absorb CO_2 from the feed gas at high pressures (i.e. from 2.07 to 13.8 MPa).[8] The capacity of physical diluents at low pressure decreases and they have to be replaced by chemical absorbers. Usually, the aqueous amine solution is used to capture CO_2 by chemical absorption process.[6] Even though amines are very effective in CO_2 capture thanks to high absorbing capacity, high reactivity and selectivity with CO_2, there are some severe disadvantages, i.e. high vapor pressure, emission of toxic compounds, elevated desorption and recycling costs due to high reaction heat. Moreover, since they are quite volatile, large amounts of organic amines are present in clean gas which could lead to the formation of dangerous secondary components, i.e. amides, nitramines, nitrosamines. These factors limit this technology for industrial application, therefore, more intensive research is required to mature the process.[9]

Cryogenic process uses fluids with very low boiling point to capture 99.99% of existing CO_2. This process working principle is based on different condensation and de-sublimation properties of CO_2. However, this technology is not suitable for diluted CO_2 streams since refrigeration requirement increases its operation cost.[10] Song et al. in 2018 reviewed different CCS strategies in terms of their advantages and disadvantages which are summarized in Table 1.[10] Under such circumstances, membrane-based technology which is a fast growing and environmental-friendly separation process, can be the best choice to overcome such limitations for CO_2 capture from post-combustion gas stream.

Table 1: Advantages and disadvantages of different CCS strategies[10]

CCS strategy	Advantages	Disadvantages
Pre-combustion	- High CO_2 concentration (~45 vol%) and elevated pressure. - Commercially applicable in some industrial sectors.	- Severe operating conditions (15–20 bar and 190–210 °C). - Excessive energy penalty due to sorbent regeneration.
Oxy-fuel combustion	- Lower capital cost - High CO_2 concentration (80–98%)	- Lower efficiency. - Higher energy penalty due to ASU*
Post-combustion	- Straightforward approach to be retrofitted - More mature than other strategies	- Dilute CO_2 concentration (5 – 15 vol%) at near atmospheric pressure

*ASU corresponds to Air Separation Unit.

Membrane based operations have the potential to replace conventional energy-intensive technologies and provide reliable solutions for CCS. A membrane is a selective barrier that separates two fluid phases and allows the selective permeation of solutes from one side of the barrier to the other. The cause of a transport through a membrane is a difference in chemical potential between both sides. This difference may be due to a gradient in temperature, (partial) pressure, concentration, or electrical potential. The mechanisms for transport strongly depend on membrane morphology. Two typical morphologies can be distinguished: porous and dense. In porous membranes the transport occurs through the empty spaces (pores) in the membrane instead

of the material itself. Whereas transport in dense membranes is described by the solution-diffusion model where, the permeability (usually expressed in Barrer units, 1 Barrer= 10^{-10} $(cm^3 \cdot cm)/(cm^2 \cdot s \cdot cm\ Hg)$) of a component is related to its diffusivity (D) and solubility (S) in the membrane material.[11] The second important characteristic of dense membranes is the selectivity, defined as the ratio of the pure permeabilities of two components. Its value gives an indication of the separation efficiency of the membrane.[12] Gas flux across the membranes can be calculated by Fick's law (Equation 1).

$$Flux\ J_i = \frac{P_i^*}{\delta} A_m \Delta P \qquad (1)$$

Where, P_i^* is permeability of component I through the membrane, δ is the thickness of the membrane, A_m is membrane area, and ΔP is pressure gradient across the membrane

Summarizing, the performance of dense membranes is strictly material dependent, while the performance of porous membranes is morphology and material dependent.[13] Membrane separation process differs based on the separation mechanisms and size of the separated particles, including microfiltration, ultrafiltration, nanofiltration, reverse osmosis, electrolysis, dialysis and gas separation. Membrane process has shown great potential in the industrial applications due to its low energy consumption, operation flexibility and simplicity, good stability, easy control and scale-up. Transport phenomenon through membrane is shown schematically in Figure 2.

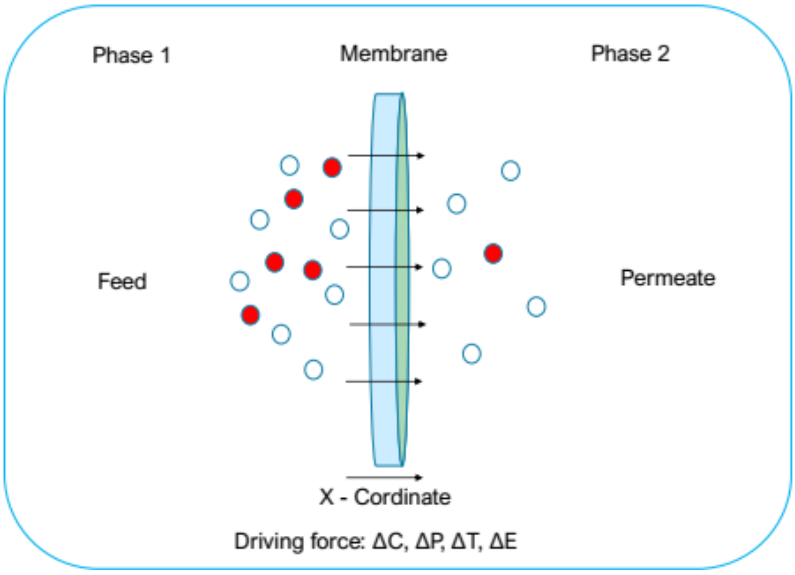

Figure 2 Schematic representation of transport phenomenon through membranes

Even though, there are different types of membranes available including: polymeric membranes, mixed matrix membranes (MMMs), thermal-rearranged membranes (TR-membranes), inorganic membranes (e.g. carbon membranes, metal-organic framework (MOF) membranes and zeolite membranes) and facilitated transport membranes etc., only few of them are compatible for gas separation application.[1] Gas mixtures can be effectively separated by synthetic membranes made of polymers or ceramic materials. Theoretically CO_2 is separated whenever there is a pressure gradient between both sides of the membrane.[5] Membranes can selectively separate for example CO_2/N_2 mixtures from flue gas based on selective permeation related to the intrinsic polymer property - permeability. In general, gas separation membranes are preferred over gas adsorption membranes for CO_2 capture since CO_2 possesses higher permeability than other constituents of flue gas.[14] Permeability can be manipulated either pressurizing the feed side or applying vacuum on the permeate side, sometimes using both but the challenge is to have high permeability without losing selectivity. Selectivity (CO_2/N_2) can be defined as permeability of CO_2 over permeability of N_2 under experimental conditions. Selectivity is very important parameter which reflects how efficient the membrane material is to selectively separate two components from the mixture. To summarize, both permeability and selectivity are intrinsic properties of membranes which coherently depend on membrane materials and working conditions. Instead of permeability and selectivity, there are another important characteristic property called "permeance" – a practical reflection of actual gas transport rate through the membrane, is defined as ratio of permeability to membrane thickness. Permeance is expressed as gas permeation unit (GPU, 1 GPU= 10^{-6} $cm^3(STP)/(cm^2 \cdot s \cdot cm\ Hg)$).[4] When the membrane thickness considered is 1 μm, permeability and permeance are the same value.

Although only 10% of share of CCS is covered by membrane based process, researchers are moving on to produce promising membranes by modifying existing one to improve its compatibility at different challenging conditions with satisfactory performance.[1] Even though polymeric membranes are economically and technologically attractive, they are bounded by their performance, known as the Robeson upper bound, where permeability is sacrificed for selectivity and vice versa as represented in Figure 3. Another main challenge of membrane technology for industrial application is higher membrane surface area required for the expected separation. It is estimated that a 600-MWe coal-based power plant need 1 million square meter membrane area to

capture evolved CO_2. To ensure that, thousands of conventional membrane modules are required in series.[9]

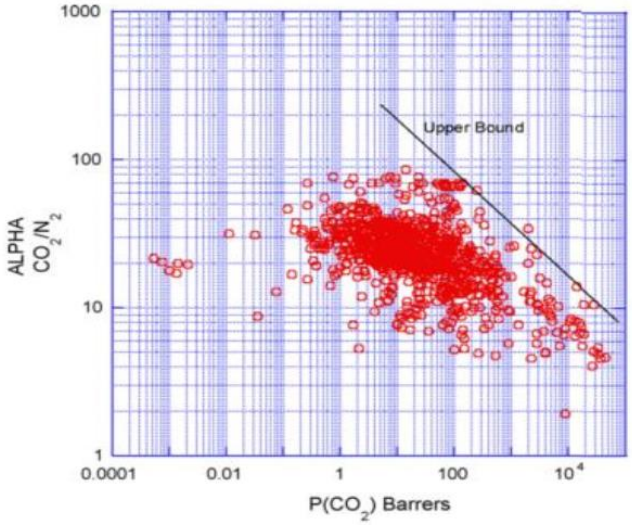

Figure 3 Robeson plot explaining trade-off between selectivity and permeability. Taken from[15]

Moreover, polymeric membranes are characterized by chemical and mechanical instability at elevated temperature, swelling phenomenon and short life-time.[14] Nevertheless, both glassy and rubbery polymers are found to be promising for gas separation application because of their high permeability and selectivity. An amorphous polymer having glass transition temperature (Tg - transition point between glassy and rubbery state) at or above room temperature is called glassy polymer while, a polymer with Tg bellow room temperature is rubbery. Polymers bellow their Tg behave like rigid glassy polymers which contain lower fraction of free volume resulting in lower permeability compared to rubbery state. Glassy polymers mostly contain closed and non-interconnected pores which allows small gas molecules to pass through and that leads to better selectivity.[12] A set of such glassy polymers are for example: polysulfone (PSF), polyethersulfone (PESF), polyetherimide (PEI) and polyimide (PI) etc. in addition rubbery polymers i.e.- Pebax® MH 1657, Pebax® 2533 etc. are found to be applicable as supportive matrix in MMMs. In contrast, inorganic membranes show better performance but difficulties in workability at the same time.[16] Membrane inorganic materials have expanded into the use of zeolites, perovskites or metal organic frameworks due to their strong thermal and chemical resistance as well as high tunability leading to increased permeability and selectivity. Furthermore, it is also possible to reduce the membrane surface area needed for high separation by increasing permeability and selectivity of

membranes which require more intensive research. A class of dense membranes named MMMs with specific fillers coupled with other existing processes (cryogenic/absorption) can be the best candidate for such perspective.

MMMs are materials made of polymers (matrix) whose properties can be modified with different compatible inorganic fillers. Unlike polymeric membranes, gas molecules permeate through MMMs by a different mechanism which is defined to be coupled with absorption and diffusion process under certain driving force i.e.- pressure gradient.[17] Micro/nano sized fillers are placed in the micropores of polymeric materials to make an efficient CO_2 capturing kit. Matrix and filler may have different flux and selectivity but produced membrane will receive superior properties than any of them.[14] MMMs are also more mechanically, thermally and chemically stable than bare polymeric membranes, so they are found to be compatible and applicable in aggressive environment.[18] Available inorganic fillers for MMMs formulation are silica, zeolite, activated carbon, etc. Some conventional polymer-zeolite pairs for MMMs can be listed as polydimethylsiloxane-silicalite, polyimide-carbon molecular sieve, polyimide-silica, nafion-zirconium oxide, HSSZ-13-polyetherimide, acrylonitrile butadiene styrene-activated carbon etc.[3,19–21] Permeability of gases through MMMs depends on intrinsic compatibility between polymer-filler pair, confirmed by proper selection of organic matrix and inorganic filler. Defects arise because of poor interface contact between incompatible pair which can be overcome by introducing new type of filler named MOF (consists of both organic and inorganic components). One of the main problems of MMMs with different organic linker than MOF is the formation of voids at the interface because of the poor affinity between the inorganic and organic phase, thus lowering the selectivity of the membrane and therefore causing it to underperform. Although MMMs provide better properties than bare membrane, finding such compatible fillers is still a challenge. Theoretically, permeability of MMMs can be calculated using Maxwell's equation as mentioned in Equation (2) with an assumption of uniform distribution of particles; afterwards the values can be compared with real-time practical results.

$$P_{MMMs} = Pc\frac{Pd + 2Pc - 2\emptyset(Pc - Pd)}{Pd + 2Pc + 2\emptyset(Pc - Pd)} \qquad (2)$$

Where, Pc is the permeability of the bare polymeric matrix, Pd is the permeability of the dispersed phase (i.e. MOFs), and $\emptyset$ is the volume fraction of the dispersed phase.[22]

Maxwell's model is helpful in pre-selection of membrane materials. Diluted filler concentration ($0 < \Phi < 0.2$) produces better performance in terms of both permeability and selectivity. Although there are five possible morphologies of membranes (the ideal, void, rigidified, pore blocked, and agglomeration combined with pore blocking) depending on interaction between polymer matrix and filler, ideal case is preferable because of its easiness to solve. Moreover, the membrane performance is morphologies dependent i.e.- voids in MMMs results from low filler dosing which leads to higher permeability without significant alteration of selectivity, rigidification is a result of high filler dose which leads to intensified selectivity but a compromise of permeability, and on further pore blocking, loss of permeability is intensified but selectivity can be higher than pure polymer membrane.[23] Moreover, a modification of the proposed ideal Maxwell's model is recommended if MMMs deviates from its ideality.[23]

MOFs are a growing class of crystalline and porous (porosity of around 90 %) materials combining a property of inorganic (metal ions as cluster) and organic (linker) materials.[18] They are formed by self-assembly of complex subunits forming 1D, 2D or 3D structures. They are characterized by high surface area (beyond 6000 m^2/g) and porosity as well as low density, and flexibility in pore size, structure and shape. Additionally, they offer tunable pore size and adjustable surface properties which made them a highly recommended candidate for CCS applications which must ensure clean energy and environment. MOFs can be synthesized by many routes including microwave, ultrasonic, electrochemical and mechanochemical.[18] Design and synthesis of MOFs depend on its application, which is the eternal aspiration of research for material scientists. MOFs are found to be compatible in a wide range of applications that include capture and storage of gas for clean energy, membrane separation, catalysis, chemical sensing (optical or ferroelectric MOFs) and biomedicine.[24]

CO_2 capture from flue gas with MOFs is the cutting-edge research field in the recent years. First MOFs based MMMs were reported in 2009.[25] Common MOFs available for MMMs based gas separation application include zeolitic imidazolate frameworks (ZIFs), materiaux de l'Institute Lavoisier (MILs), MOF-5, MOC-4, HKUST-1, etc. Atomic structure of such MOFs is shown in Figure 4. Chemical formulae of MOFs are reported as Zn-O (IRMOF-1), Cu-O (HKUST-1), Al-O (MIL-53, MIL-101), and Zn-N (ZIF series). Among all possible MOFs, ZIF series (ZIF-8, ZIF-

11, ZIF-53, ZIF-90, ZIF-94, ZIF-95, ZIF-100, etc.) are considered to be most stable since they can sustain their crystal structure even at boiling point of a solvent (benzene and water).[26]

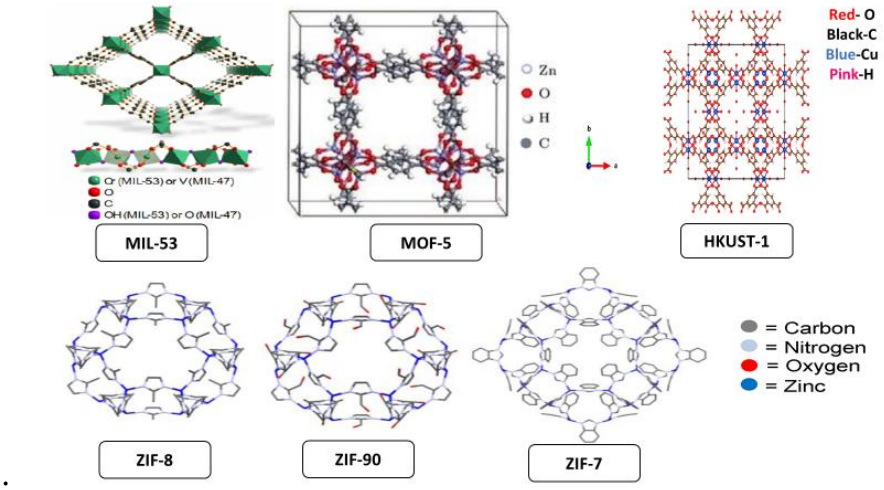

Figure 4: Structure of different Metal Organic Frameworks (MOFs). Taken from[27–31]

Moreover, in the case of using MOFs as membrane fillers, the in-build organic ligands may improve the filler-polymer interaction, avoiding the presence of non-selective micro-gaps without blocking access to the surface. However, an agglomeration of dispersed phase is noticed at higher loading of MOF which increases diffusion distance between particles resulting in membrane underperformance.

ZIFs are a class of MOFs that exhibit a zeolite type structure. They are characterized by exceptional chemical and thermal stability (up to 400 ^{o}C), high microporosity, and large surface area. ZIFs are composed of a divalent metal cation (i.e. Co^{2+} or Zn^{2+}) that is linked to the nitrogen atoms which are part of a deprotonated imidazole molecule creating tetrahedral frameworks. The stability combined with their microporous structures makes them very attractive for gas separation.

ZIF-94, also known as SIM-1, as shown in Figure 5, is a type of ZIF and is an analogue to extensively studied ZIF-8.[32] It possesses an SOD topology, well distributed and defined 3D pore network with 2.6 Å diameter.[19] It is highly selective for gas separation due to its high CO_2 capture ability even at lower operating pressure.[19] This structure is found to be stable at elevated

temperature. It can be synthesized with cluster (zinc acetate) to binder (imidazole) ratio 1:1.7 with proper reaction and washing conditions.

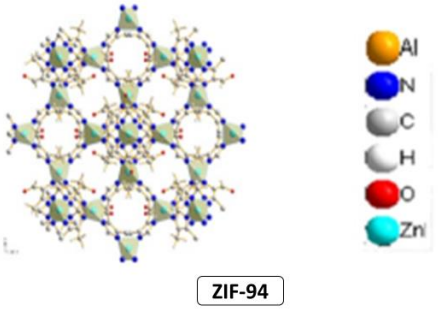

Figure 5: Structure of ZIF-94. Taken from.[19]

Polyamide-b-ethylene oxide, or commercially known as Pebax, is a block copolymer containing blend of two monomers: i) soft polyethylene oxide (PEO) domain along with ii) hard and crystalline polyamide (PA) segment. The hard domain served as a support to PEO and inhibit its crystallization.[33] Since this polymer consists of both glassy and rubbery segments, it provides high gas permeation without loss of selectivity and mechanical stability of a thin film. There are different subclasses of Pebax polymers which are synthesized by altering PEO and PA compositions where an increase of PEO portion significantly upgrades solubility of polarizable gases.[34] Pebax® MH 1657 is a commercial rubbery and thermoplastic polymer that is a subclass of Pebax. It offers good thermal (melting point of 204 °C) and mechanical property without losing the permeability and selectivity. Figure 6 represents molecular structure of commercial Pebax® MH 1657.

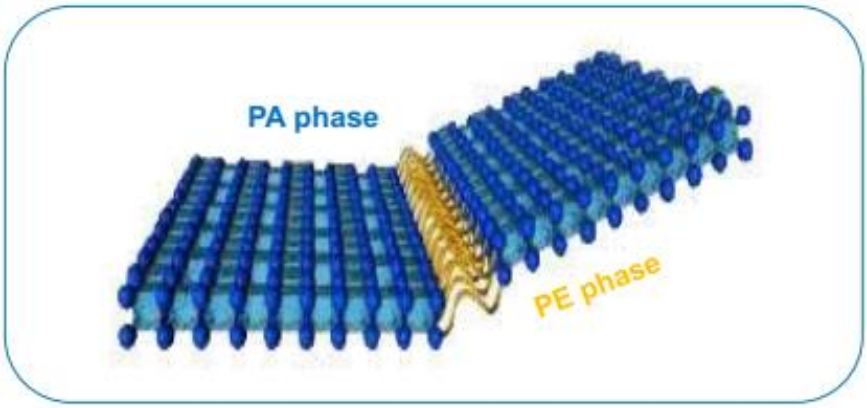

Figure 6: Structure of Pebax® MH 1657. Obtained from Arkema, France.

Because of its higher melting point, Pebax has found applications in gas separation especially in MMMs as a matrix support at elevated temperatures. Pebax® MH 1657 is very attractive especially for polar gas separation, such as CO_2, from nonpolar light gases, such as N_2, since PEO offers better affinity to polar gases.[35] Additionally Kim et al. (2001) compared characteristics of four types of Pebax codes (2533, 3533, 4033 and 1657), and they finally confirmed that Pebax® MH 1657 shows a significant selectivity (polarizable/nonpolar gas).[36]

2 Objectives

It was decided that to increase the CO_2 capture even more, ZIF-94 will be added to the polymeric matrix mainly because it is characterized by high CO_2 uptake at low pressure. Hence, the objectives of this research is to use ZIF-94 as a better MOF candidate in MMMs to capture CO_2 from post-combustion flue gas where commercial Pebax® MH 1657 is being used as a polymer matrix. The work will be devoted to finding the best possible combination of MOF and polymer taking into account different MOF loadings into the matrix as well as various concentrations of polymer in the solvent. The fabricated membranes will be characterized and tested by gas chromatography in order to estimate their gas separation (CO_2 over N_2) performance.

3 Experimental procedure

3.1 Materials

For lab scale ZIF-94 synthesis, zinc acetate dihydrate and 4-methyl -5- imidazolecarboxaldehyde were purchased from Acros Chemicals (98% and 99% purity respectively). Methanol (99.8%) was obtained from Scharlau, Spain and anhydrous Tetrahydrofuran (≥99.9%) were obtained from Sigma-Aldrich. Commercially available PEBAX-1657 was obtained from Arkema, France.

3.2 Methodology

3.2.1 Synthesis of ZIF-94

ZIF-94 was synthesized by two step process in the laboratory of CREG (Catalysis, Molecular Separations and Reactor Engineering Group) at the Chemical and Environmental Engineering Department and Institute of Nanoscience of Aragon of the University of Zaragoza. Initially, 528 mg (2.82 mmol) of zinc acetate dihydrate was dissolved in 2 mL of 99.8% methanol (MeOH). On the other hand, 528 mg (4.75 mmol) of 4-methyl-5-imidazole carboxaldehyde was dissolved in 5 mL of THF. Next, the methanol solution was added to the THF solution under vigorous mixing.

Afterwards, the mixture was stirred for 16 h at room temperature (RT). The product was collected by centrifugation with MeOH at 10000 rpm for 10 min (the process was repeated for three times). The resulting ZIF-94 was dried in air overnight under RT. Finally, ZIF-94 was ready for characterization and application for MMM preparation and subsequent gas separation performance testing. Schematic representation of the synthesis of ZIF-94 is shown in Figure 7. A summary of the chemicals used for ZIF-94 synthesis with their molar ratio are represented in Table 2.

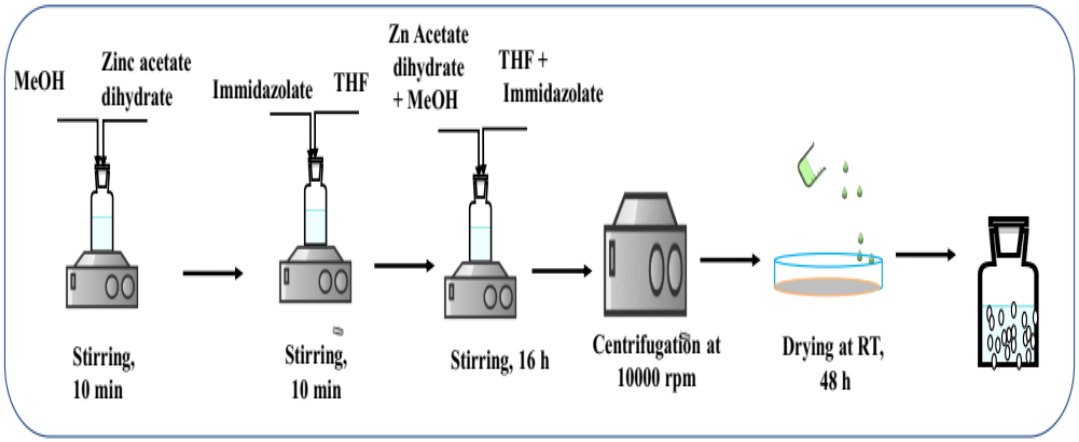

Figure 7: Sketch of synthesis of MOF ZIF-94.

Table 2: List of chemicals being used and their respective molar ratio.

Chemicals	***Added quantity***	***Absolute quantity (mg)***	***No. of mmol***	***Molar ratio (Metal: Ligand: MeOH: THF)***
Zinc acetate dihydrate	528 mg	518	2.82	
Immidazole	528 mg	523	4.75	**1:1.7:17:22**
MeOH	2 mL (99.8%)	1579	49	
THF	5 mL (99.9%)	4440	62	

3.2.2 Fabrication of mixed matrix membranes (MMMs)

The MMMs are prepared following a two-step process. First, different concentrations of Pebax® MH 1657 were dissolved in a mixture of EtOH/water (70/30 (v/v)) by stirring under reflux at 80 °C for approximately 1 h. In the meantime, the required dose of ZIF-94, that depended on the loading that was needed, was dissolved in 1.5 mL of EtOH/water (70/30) mixture by repeated

sonication and stirring at RT. Next, both solutions were mixed and kept for overnight stirring at RT. In the extension of the fabrication process, the solution was poured on a Petri dish (PDC) or cast by a casting knife (CK) (Elcometer 4340 Automatic Film Applicator). At the end of the process, the membranes were dried for 48 h in a top-drilled box under a solvent-saturated atmosphere at environmental conditions. Schematic representation of fabrication of MMMs is shown in Figure 8. Additionally, bare membrane (without ZIF-94) for all composition of Pebax® MH 1657 were also casted to compare its performance against MMMs.

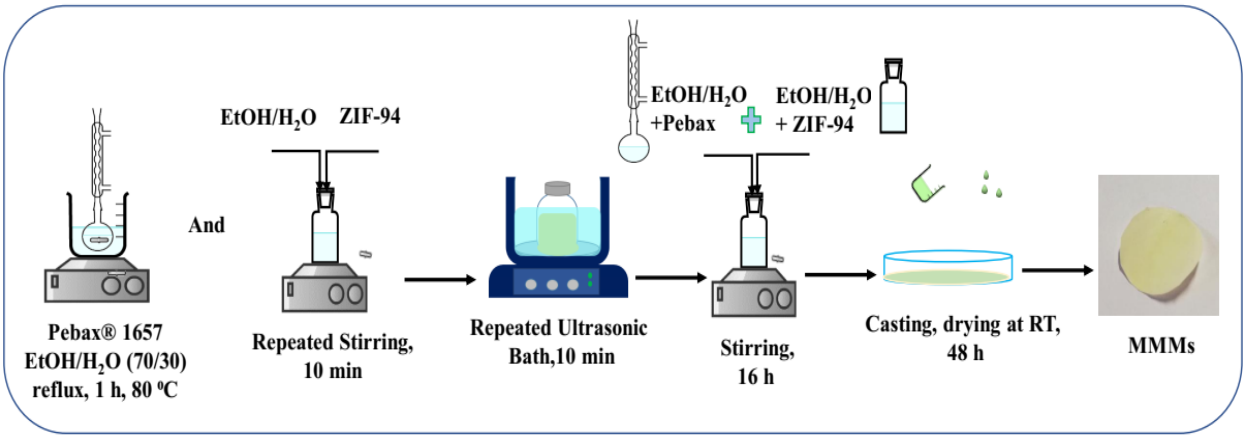

Figure 8: Schematic representation of fabrication of MMMs.

3.3 Characterization

Characterization of synthesized ZIF-94 and MMMs is important to do before applying them for gas separation application. Several instruments were adopted for successful characterization of fabricated materials. Scanning electron microscopic (SEM) analysis confirms shape and particle size distribution of synthesized ZIF-94 and its homogeneity of distribution in MMMs. Brunauer-Emmett-Teller (BET) specific surface area is an important parameter which is correlated with gas adsorption capacity. Thermal gravimetric analysis (TGA) indicates thermal stability of both ZIF-94 and MMMs within a wide band of temperatures which helps to select them for specific applications as well as ensure the purity of a material. X-ray diffraction (XRD) confirms crystallinity of ZIF-94. When all the parameters are specified, prescribed MMMs are ready to be incorporated into the gas separation module to check their performance in terms of permeability and selectivity. Detailed demonstration of the analytical instrument is represented in the section bellow.

3.3.1 Scanning electron microscopy (SEM)

The morphology of synthesized ZIF-94, as well as surface and cross-sectional morphology of Pebax® MH 1657 bare membrane and Pebax® MH 1657 + MOFs based MMMs were inspected by scanning electron microscopy (SEM) with back scattered electron mode using an Inspect F50 model scanning microscope (FEI), operated at 10 kV. SEM images reveal particle size and shape of the particulate materials. Additionally, images can be further analyzed using ImageJ software to investigate particle size distribution of the materials under investigation.

3.3.2 Thermogravimetric analysis (TGA)

Thermogravimetric analysis was carried out using a Mettler Toledo TGA/STDA 851e. Small pieces of membranes (approx. 5 mg) placed in 70 μL alumina pans were heated under an air flow (40 mL min^{-1}) from 35 to 700 ºC at a heating rate of 10 ºC min^{-1}. Loss of wt.% as a function of temperature is revealed from TGA analysis which is characteristic of removal of solvents and thermal degradation of the sample under investigation. This information is very helpful to select materials for industrial application, especially in aggressive environmental condition of flue gas.

3.3.3 BET specific surface area

The N_2 adsorption-desorption isotherms were obtained using Micrometrics Tristar 3000 at 77 K. Before these measurements, the samples were degassed for 8 h under vacuum at 200 ºC using a heating rate of 10 ºC min^{-1}. BET analysis provides specific adsorption volume of porous materials as a function of relative pressure (i.e. and isotherm). The N_2 adsorption-desorption isotherms are also helpful to confirm type of porous materials (microporous or macroporous).

3.3.4 X-ray diffraction

Membranes and nanoparticles were also characterized by X-ray diffraction (XRD) using a Panalytical Empyrean equipment with CuK_α radiation ($\lambda = 0.154$ nm), over the range of 5º- 40º at a scan rate of 0.03º s^{-1}, to examine the *d*-spacing of the nanoparticles and membranes. These XRD analyses enable to confirm crystallinity of the porous materials as well as to confirm the purity of the crystalline phase.

3.3.5 Gas chromatography (GC)

The separation of the CO_2/N_2 mixture was performed in the experimental system that is schematically presented in Figure 9. The membranes were cut and placed in a module consisting

of two stainless steel pieces and a 316LSS macroporous disc support (Mott Co.) with a 20 μm nominal pore size. Membranes, 2.12 cm^2 in area, were gripped inside with Viton O-rings. To control the temperature of the experiment, which influences gas separation, the permeation module was placed in an UNE 200 Memmert oven. Gas separation measurements were carried out by feeding the post-combustion gaseous mixture of CO_2/N_2 (15/85 cm^3(STP) min^{-1}) at an operating pressure of 3 bar and 35 °C) to the feed side, controlled by two mass-flow controllers (Alicat Scientific, MC-100CCM-D). The permeate side of the membrane was swept with 2 cm^3(STP) min^{-1} of He, at atmospheric pressure (approx. 1 bar) (Alicat Scientific, MC-5CCM-D). Concentrations of N_2 and CO_2 in the outgoing streams were analyzed online by an Agilent 3000A micro-gas chromatograph. Permeability was calculated in Barrer (10^{-10} cm^3 (STP) cm cm^{-2} s^{-1} cm Hg^{-1}) once the steady state of the exit stream was reached (at least after 3 h). The separation selectivity was calculated as the ratio of permeabilities (Equation (3)). Afterward, permeance in GPU (10^{-6} cm^3 (STP) cm^{-2} s^{-1} cm Hg^{-1}) can be calculated as per Equation 4 with the permeability in Barrer and the membrane thickness in μm.

$$Selectivity = \frac{Permeability\ of\ CO_2}{Permeability\ of\ N_2} \quad (3)$$

$$Permeance = \frac{Permeability\ of\ CO_2}{Membrane\ thickness} \quad (4)$$

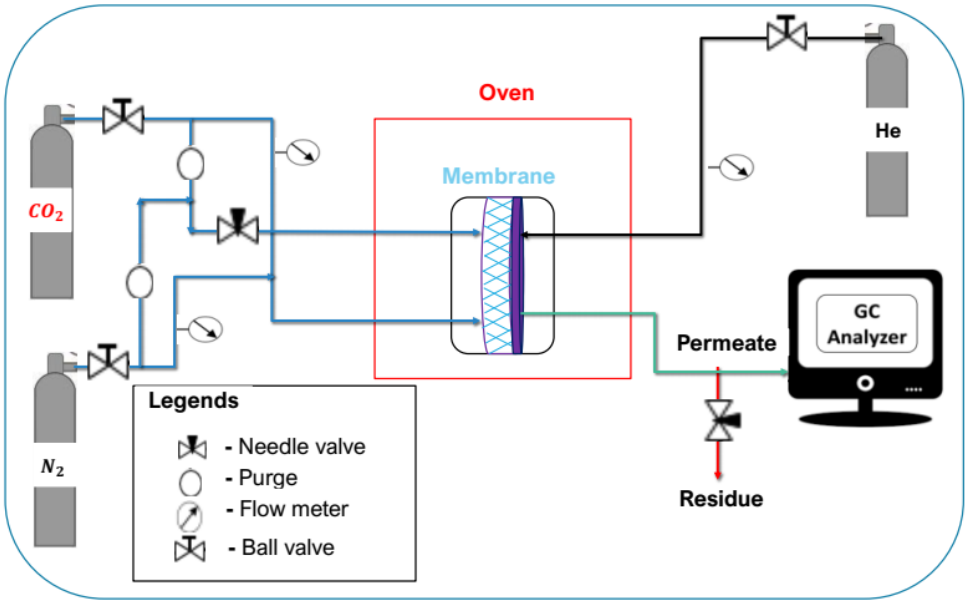

Figure 9: Gas permeation experimental system.

4. Result and discussion

4.1 Characterization of ZIF-94

ZIF-94 was characterized by various techniques as mentioned in the section 2.3. SEM analysis confirmed homogeneous distribution of the synthesized ZIF-94 particles represented in Figure 10 (A). It also revealed an average particle size of 175 ± 68 nm. Particle distribution bar graphs in Figure 10 (B) also show that the majority of the particles ranged from 100 nm - 200 nm.

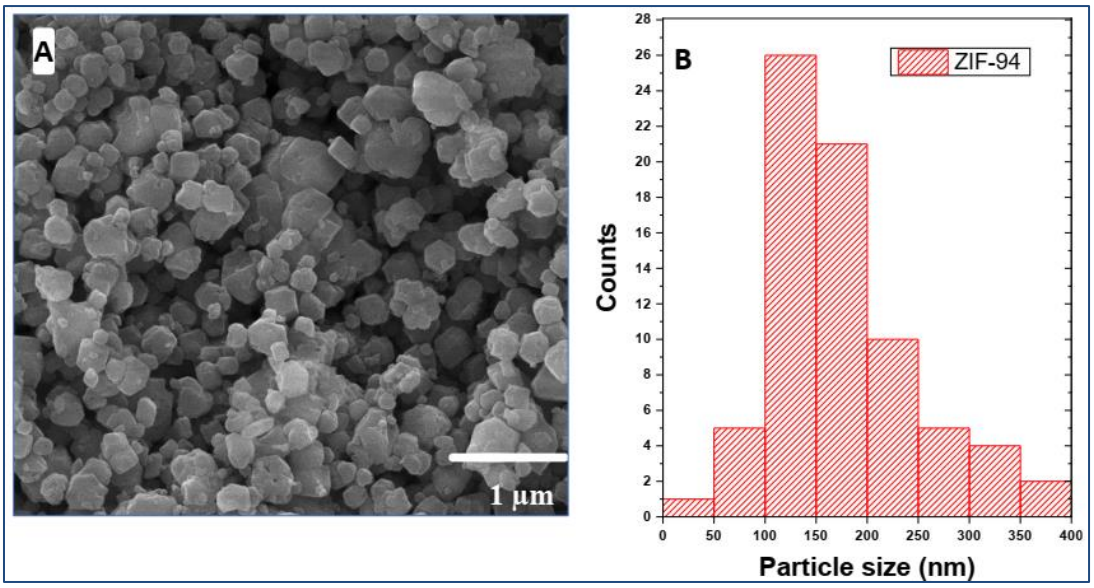

Figure 10: SEM image of synthesized ZIF-94 (A) and Particle size distribution (B)

X-ray diffraction pattern allowed to determine the crystallinity, purities of the product and its crystal phases. Figure 11 shows that the ZIF-94 synthesized corresponds to the simulated CIF data of ZIF-8. Relative intensity and peak positions match well with single crystal data corresponding to ZIF-8. Since the XRD pattern of ZIF-94 is the same of simulated CIF, other characterization techniques were helpful to corroborate the presence of ZIF-94.

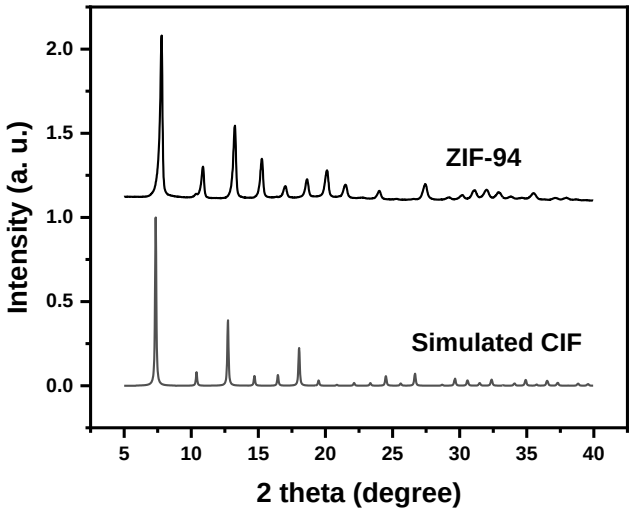

Figure 11: Comparison of XRD pattern of synthesized ZIF-94 with simulated (CIF). [40,41]

The N_2 adsorption-desorption analysis provides BET specific surface area which is one of the parameters to distinguish between ZIF-8 and ZIF-94. The BET specific surface area of ZIF-8 usually lies between 1300 to 1810 m^2/g,[37,38] while characteristic BET specific surface area of ZIF-94 is much smaller (424 - 480 m^2/g).[39] Synthesized ZIF-94 produced BET specific surface area of 317 m^2/g showed in Figure 12. Moreover, the prescribed MOF showed type I isotherm with small hysteresis. This suggests some hierarchical porosity due to the mesoposority present in between MOF nanoparticles.

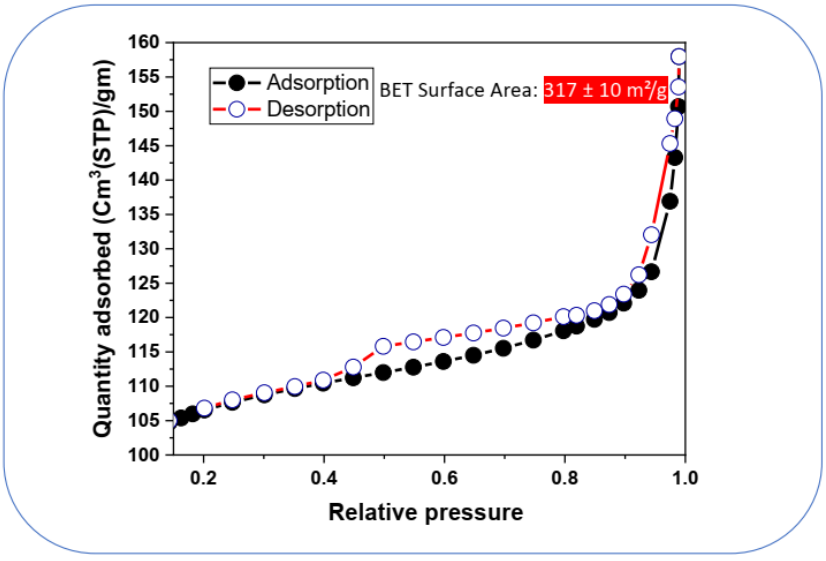

Figure 12: N_2 adsorption-desorption curve of synthesized ZIF-94

TGA curve (in the range of 35 ºC - 700 ºC with air) represents thermal behavior of synthesized ZIF-94. There are several sharp decreases of weight which significantly represents compositional properties of the material. Weight loss up to 70°C signify presence of solvent residue (MeOH) after drying at room temperature. Further weight reduction in the range of 70 - 130 °C represents loss of solvents from internal pores of ZIF-94. Synthesized MOF is found to be stable up to approximately 350 °C. Then, it undergoes degradation which continues until 600 °C with a 71% loss of initial total weight (Figure 13). Afterwards, no significant change was observed.

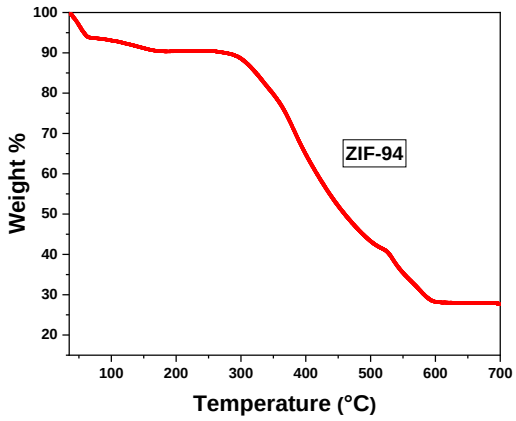

Figure 13: TGA analysis of synthesized ZIF-94

4.2 Characterization of MMMs

SEM image of a cross-section of fabricated MMM represents fine distribution of ZIF-94 through polymeric matrix (Figure 14 (B)) and it exemplifies sharp difference from bare polymeric Pebax membrane shown in Figure 14 (A).

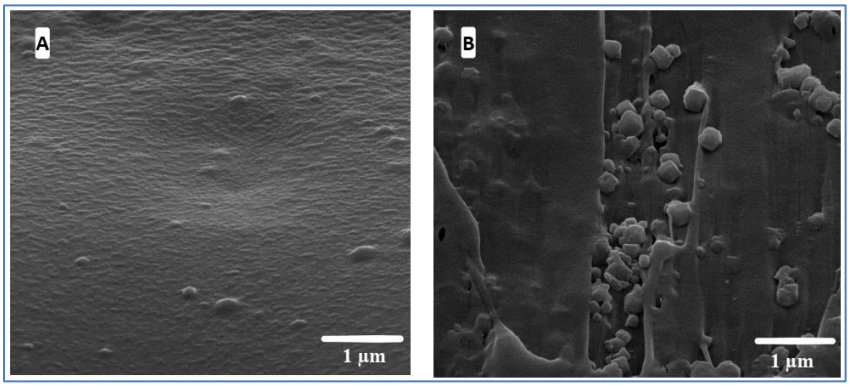

Figure 14: Cross section SEM imaging (50000 x) of bare membrane (A), MMM (12% Pebax® with 20% ZIF-94) high magnification (50000 x) image (B).

TGA analysis of bare polymeric Pebax membrane and MMMs were also investigated (shown in Figure 15). There was an unknown technical error while TGA measurement of bare membrane (revealed from TGA curve) which should be repeated before concluding its comparison against MMMs.

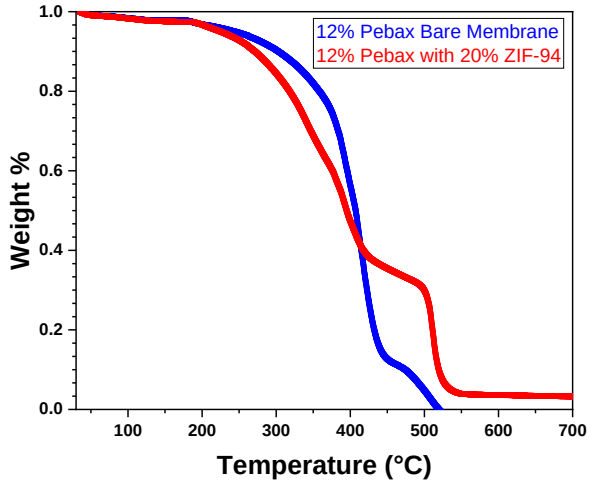

Figure 15: TGA analysis of bare Pebax polymeric membrane and comparison with MMMs.

4.3 Membrane performance analysis

MMMs were fabricated with 6 wt.% Pebax® MH 1657 as matrix and various ZIF-94 doses (as filler) by two different methods (casting knife (CK) and Petri dish casting (PDC)) which were analyzed for their performance over CO_2/N_2 separation and compared. The performance of bare polymeric membrane was initially measured and next the loading of ZIF-94 was gradually increased from 5 wt.% to 25 wt.%. Figure 16 (A) shows that knife casted membranes provide better permeance but CO_2/N_2 selectivity was very poor. On the other hand, membrane cast by PDC produced better selectivity but poor permeance (Figure 16 (B)). This suggests that there is always a trade-off between both parameters. Since the membranes casted by CK were very thin (maximum thickness was obtained 16 µm, given in Appendices-1) it was very difficult to manage them and therefore the values of permeance and selectivity were not consistent. Moreover, it is possible that these membranes possessed some micro defects which reduced selectivity and produced higher permeance. Hence, Petri dish casting method was preferred over knife casting for further experimental analysis expecting fewer micro defects.

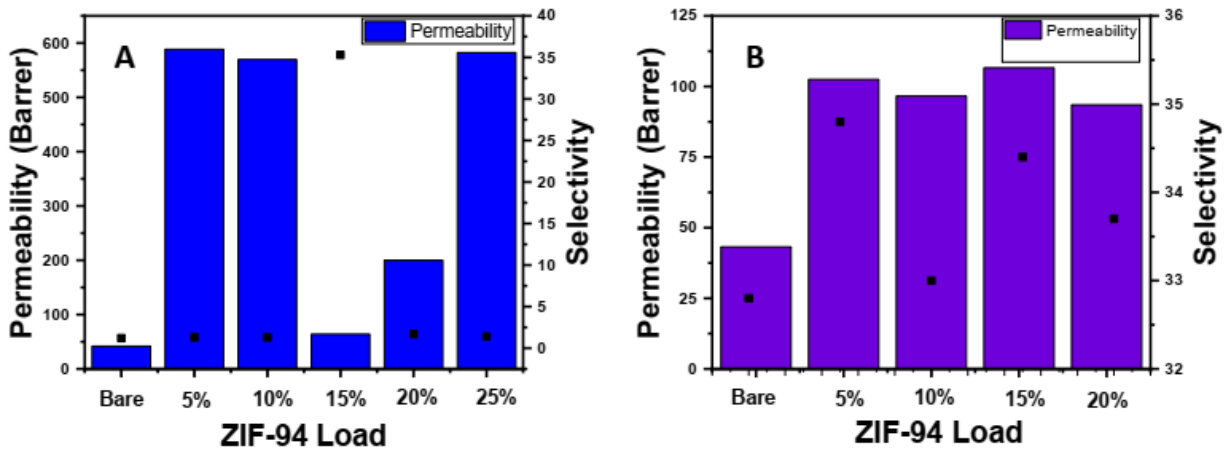

Figure 16: Performance of MMMs (6 % wt. Pebax® MH 1657 + various -MOF loading) (A is for knife casting) and (B is for petri dish casting) for post combustion gas separation

Other Pebax® MH 1657 matrix compositions (9% and 12% by wt.%) were also investigated using Petri dish casting in search of better results. Figure 17 (A) represents the performance of MMMs having 9 % wt. of Pebax® MH 1657 and various MOF loadings from 5 to 25 wt.%. In such attempt, the best results in terms of selectivity (43.5) were obtained for 10 wt.% load of ZIF-94; however, the permeance was very low 1.5 GPU (permeability 127 Barrer considering the corresponding membrane thickness of 84 μm) (Figure 17 (A)). Further increase in MOF dose was found to decrease selectivity down to 30.8 whereas the permeance was not significantly changed unless the case of 25 wt.% filler loading which produced permeance of 53.3 GPU (permeability 2930 Barrer considering the corresponding membrane thickness of 55 μm) with a CO_2/N_2 selectivity of 30.8 (Appendices -2). Additionally, MMMs having 12 % Pebax matrix were casted and evaluated for permeation analysis shown in Figure 17 (B). It revealed that, the 5 %wt. loading of MOF yields to best permeance (for the composition), equal to 151 GPU (permeability 529 Barrer considering the corresponding membrane thickness of 151 μm) and a CO_2/N_2 selectivity of 37.4. Further increase of ZIF-94 loading in 12 wt.% Pebax® MH 1657 produces lower selectivity and permeance but they still outperformed the bare Pebax membrane (Appendices -3). Further intensive research is required to optimize Pebax® MH 1657 concentration as well as MOF loading to obtain the highest selectivity and permeance (to surpass the Robeson limit, see Figure 18) without sacrificing the mechanical stability of the MMMs.

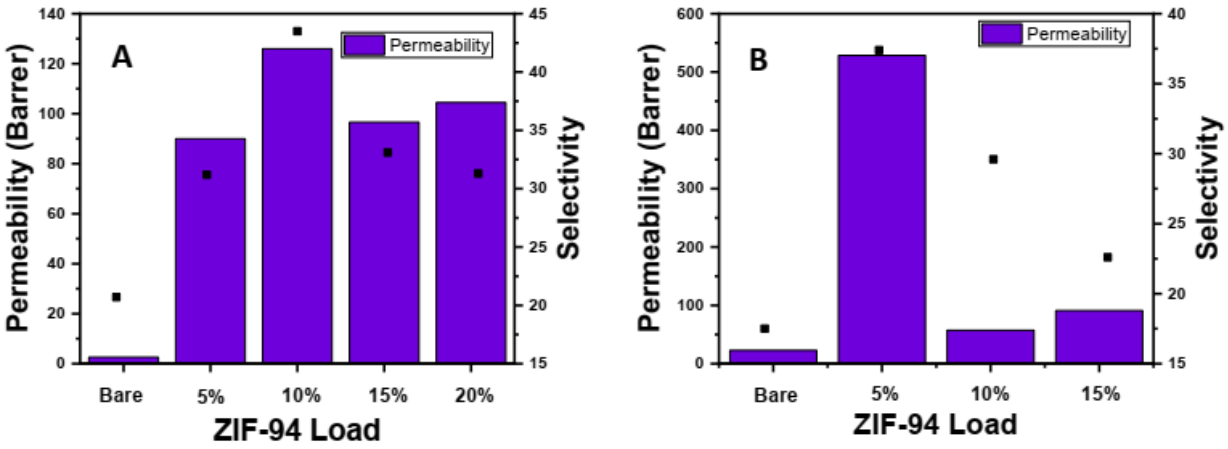

Figure 17:Performance of MMMs, (A) at 9 wt.% and (B) 12 wt.% of Pebax® MH 1657 with different MOF dose

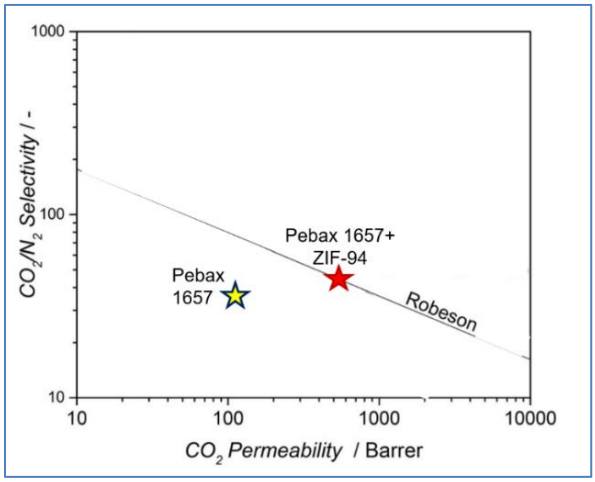

Figure 18: Robeson plot and finding of this research. Red star corresponds to the best results obtained so far (9 wt.% Pebax + 10 wt.% ZIF-94)

Justification of revealed performance of fabricated MMMs with Maxwell's equation for theoretical estimation is presented in Table 3. It is clearly evident that, in most of the cases, experimental performance is much higher. The possible reasons behind can be extrapolated as homogeneous distribution of filler is difficult to be assured while fabrication which is an indispensable assumption of the theory. Additionally, there are possibility of micro-defects in the membrane which has impact on permeability as well. Although, MMMs fabricated with 9 % and 12 % Pebax matrix overperformed bare membranes, the reproduction of the results is mandatory before making any announcement. So, reproduction of the results is the new goal of the project.

Table 3: Comparison of theoretical (according to Maxwell's equation) and practical permeability for CO2 (Barrer)

Pebax@ dose (%)	***Filler dose***	***P_c (CO_2)***	***P_d (CO_2) (Average)***	***P_{MMMs} (CO_2) (Theoretical)***	***P_{MMMs} (CO_2) (Practical)***
	0.05	30.0		33.9	103
6%	0.10	30.0		38.4	96.6
	0.15	30.0		43.6	107
	0.20	30.0		49.6	93.5
9%	0.05	2.6	175	3.2	2.6
	0.10	2.6		3.9	126
	0.15	2.6		4.8	96.6
	0.20	2.6		5.9	105
12%	0.10	22.9		30.2	57.4
	0.15	22.9		34.8	91.2

4.4. Reproduction of MMMs

MMMs of different composition were refabricated to reproduce previous performances and recent results are shown in Figure 19. The obtained results revealed no consistency of membrane performance. Repetition of 9% Pebax with 10 % ZIF-94 loading produced three different results in separate attempts. More importantly, reproduced performances are much lower than previously obtained results, a comparison is represented in Figure 20. Surprisingly, all re-casted membranes performed lower in terms of selectivity compared to 6 % bare polymeric membrane. Whereas considering both permeability and selectivity, MMMs are better than any of the bare Pebax membrane. On the other hand, 9% Pebax based MMMs better performed compared to 9 % bare polymeric membrane. Here, an average of the three repetitions are considered to compare with previous results. Comparison of recent and previous results are represented in table 4. Obviously, previous results are better in terms of overall performance. However, from the results that we have it is very difficult to make any final comments of MOF loading to have better performance. So more intensive research is required to conclude optimum composition of MMMs, the current master thesis being just a preliminary work.

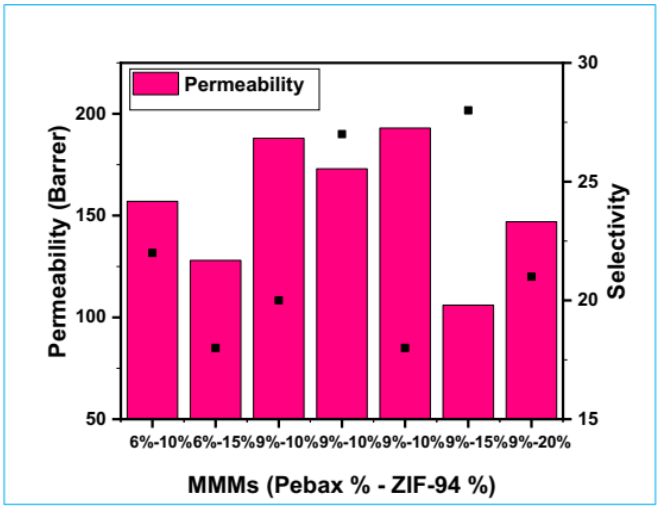

Figure 19: Performance of reproduced MMMs

Table 4: Comparison of MMMs performance with previous results

Pebax Dose (wt%)	*MOF loading (wt%)*	*Membrane thickness (µm)*	*PCO_2 (Barrer)*	*Previous PCO_2 (Barrer)*	*Selectivity CO_2/N_2*	*Previous selectivity*
6	10	71	**157**	**96**	**22**	**33**
	15	70	**128**	**106**	**18**	**34**
9	10	84	**188**	**126**	**20**	**43**
	10	64	**173**	**126**	**27**	**43**
	10	91	**193**	**126**	**18**	**43**
	15	31	**106**	**97**	**28**	**33**
	20	91	**147**	**106**	**21**	**32**

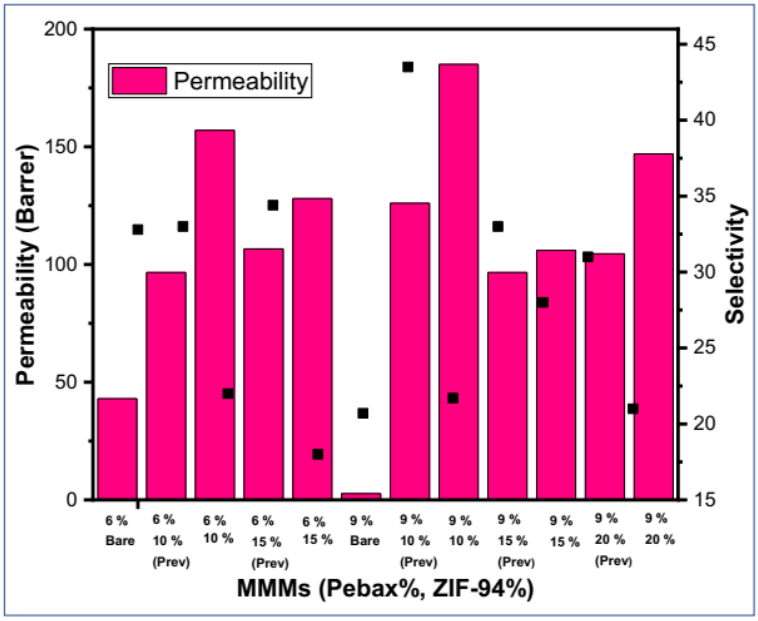

Figure 20: Comparison of reproduced MMMs performance with bare Pebax and previously obtained outputs.

Figure 21 represents error bar graph of all results where, it is clear that, membrane performance is fluctuating in a wide range. More importantly, selectivity is more fluctuating than permeability. For example, if we look at the composition (9 wt% Pebax and 10 wt% ZIF - 94) which made best result previously, it shows highest fluctuation in terms of selectivity (15 to 38) when an average is considered. Whereas fluctuation band of permeability is not that extended. Further comparison of theoretically possible CO_2 permeability with practical values (obtained for refabricated MMMs) are not identical (Table 5). Possible reasons are the same as mentioned before in section 3.3. Although, recent research focused on solving this issue, unfortunately, emergency situation because of COVID-19 become a resistance to the success.

Table 5: Comparison of refabricated MMMs in terms of their permeability (for CO2) against Maxwell's theoretical values (in Barrer)

Pebax@ dose (%)	***Filler dose***	***P_c (CO_2)***	***P_d (CO_2) (Average)***	***P_{MMMs} (CO_2) (Theoretical)***	***P_{MMMs} (CO_2) (Practical)***
6%	0.10	30.		38.4	157
	0.15	30.		43.6	128
	0.10	2.6	175	3.9	186 (avg.)
9%	0.15	2.6		4.8	106
	0.20	2.6		5.9	147

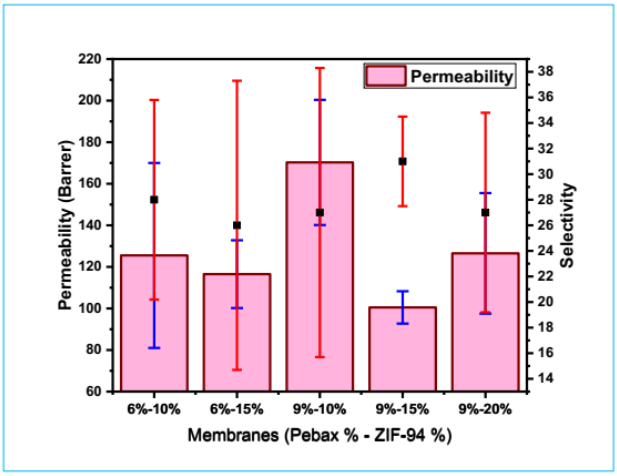

Figure 21: MMMs performance with error bar

5. Conclusions

Mixed matrix membranes (MMMs) with Pebax® MH 1657 as rubbery polymeric support and MMMs with different compositions can be an important separation element for treatment of post combustion flue gas. MMMs were successfully prepared in easiest way which could be scaled up. So far, CO_2/N_2 selectivity of 43.5 (Pebax 9 wt.% and ZIF-94 dose 10 wt.%) was obtained throughout the experiment which lies on the limit of Robeson plot (Figure 17). Attempts for reproduction of previous results are not successful yet, but further continuation after emergency is required to reach any conclusion of the project.

References

(1) Dai, Z.; Noble, R. D.; Gin, D. L.; Zhang, X.; Deng, L. Combination of Ionic Liquids with Membrane Technology: A New Approach for CO2 Separation. *J. Memb. Sci.* **2016**, *497*, 1–20. https://doi.org/10.1016/j.memsci.2015.08.060.

(2) Global CCS Institute. CO2 Capture Technologies - PostCombustion Capture (PCC). **2012**, No. January, 1–16.

(3) Yang, H.; Xu, Z.; Fan, M.; Gupta, R.; Slimane, R. B.; Bland, A. E.; Wright, I. Progress in Carbon Dioxide Separation and Capture: A Review. *J. Environ. Sci.* **2008**, *20* (1), 14–27. https://doi.org/10.1016/S1001-0742(08)60002-9.

(4) Xie, K.; Fu, Q.; Qiao, G. G.; Webley, P. A. Recent Progress on Fabrication Methods of Polymeric Thin Film Gas Separation Membranes for CO2 Capture. *J. Memb. Sci.* **2019**, *572* (October 2018), 38–60. https://doi.org/10.1016/j.memsci.2018.10.049.

(5) Ho, M. T.; Allinson, G. W.; Wiley, D. E. Reducing the Cost of CO2 Capture from Flue Gases Using Membrane Technology. *Ind. Eng. Chem. Res.* **2008**, *47* (5), 1562–1568. https://doi.org/10.1021/ie070541y.

(6) Torralba-Calleja, E.; Skinner, J.; Gutiérrez-Tauste, D. CO2 Capture in Ionic Liquids: A Review of Solubilities and Experimental Methods. *J. Chem.* **2013**, *2013*. https://doi.org/10.1155/2013/473584.

(7) Choi, W. J.; Seo, J. B.; Jang, S. Y.; Jung, J. H.; Oh, K. J. Removal Characteristics of CO2 Using Aqueous MEA/AMP Solutions in the Absorption and Regeneration Process. *J. Environ. Sci.* **2009**, *21* (7), 907–913. https://doi.org/10.1016/S1001-0742(08)62360-8.

(8) Ramdin, M.; De Loos, T. W.; Vlugt, T. J. H. State-of-the-Art of CO 2 Capture with Ionic Liquids. *Ind. Eng. Chem. Res.* **2012**, *51* (24), 8149–8177. https://doi.org/10.1021/ie3003705.

(9) Bhattacharyya, D.; Miller, D. C. Post-Combustion CO2 Capture Technologies — a Review of Processes for Solvent-Based and Sorbent-Based CO2 Capture. *Curr. Opin. Chem. Eng.* **2017**, *17*, 78–92. https://doi.org/10.1016/j.coche.2017.06.005.

(10) Song, C.; Liu, Q.; Deng, S.; Li, H.; Kitamura, Y. Cryogenic-Based CO2 Capture Technologies: State-of-the-Art Developments and Current Challenges. *Renew. Sustain. Energy Rev.* **2019**, *101* (October 2017), 265–278. https://doi.org/10.1016/j.rser.2018.11.018.

(11) Chung, T. S.; Jiang, L. Y.; Li, Y.; Kulprathipanja, S. Mixed Matrix Membranes (MMMs) Comprising Organic Polymers with Dispersed Inorganic Fillers for Gas Separation. *Prog. Polym. Sci.* **2007**, *32* (4), 483–507. https://doi.org/10.1016/j.progpolymsci.2007.01.008.

(12) Bernardo, P.; Drioli, E.; Golemme, G. Membrane Gas Separation: A Review/State of the Art. *Ind. Eng. Chem. Res.* **2009**, *48* (10), 4638–4663. https://doi.org/10.1021/ie8019032.

(13) Liang, C. Z.; Chung, T. S.; Lai, J. Y. A Review of Polymeric Composite Membranes for Gas Separation and Energy Production. *Prog. Polym. Sci.* **2019**, *97*, 101141. https://doi.org/10.1016/j.progpolymsci.2019.06.001.

(14) Mondal, M. K.; Balsora, H. K.; Varshney, P. Progress and Trends in CO2 Capture/Separation Technologies: A Review. *Energy* **2012**, *46* (1), 431–441. https://doi.org/10.1016/j.energy.2012.08.006.

(15) Robeson, L. M. The Upper Bound Revisited. *J. Memb. Sci.* **2008**, *320* (1–2), 390–400. https://doi.org/10.1016/j.memsci.2008.04.030.

(16) Wang, Z.; Wang, D.; Zhang, S.; Hu, L.; Jin, J. Interfacial Design of Mixed Matrix Membranes for Improved Gas Separation Performance. *Adv. Mater.* **2016**, *28* (17), 3399–3405. https://doi.org/10.1002/adma.201504982.

(17) Goh, P. S.; Ismail, A. F.; Sanip, S. M.; Ng, B. C.; Aziz, M. Recent Advances of Inorganic Fillers in Mixed Matrix Membrane for Gas Separation. *Sep. Purif. Technol.* **2011**, *81* (3), 243–264. https://doi.org/10.1016/j.seppur.2011.07.042.

(18) Zhou, H. C.; Long, J. R.; Yaghi, O. M. Introduction to Metal-Organic Frameworks. *Chem. Rev.* **2012**, *112* (2), 673–674. https://doi.org/10.1021/cr300014x.

(19) Tantekin-Ersolmaz, Ş. B.; Atalay-Oral, Ç.; Tatlier, M.; Erdem-Şenatalar, A.; Schoeman, B.; Sterte, J. Effect of Zeolite Particle Size on the Performance of Polymer-Zeolite Mixed Matrix Membranes. *J. Memb. Sci.* **2000**, *175* (2), 285–288. https://doi.org/10.1016/S0376-7388(00)00423-3.

(20) Kusakabe, K.; Ichiki, K.; Hayashi, J. I.; Maeda, H.; Morooka, S. Preparation and Characterization of Silica-Polyimide Composite Membranes Coated on Porous Tubes for CO2 Separation. *J. Memb. Sci.* **1996**, *115* (1), 65–75. https://doi.org/10.1016/0376-7388(95)00290-1.

(21) Apichatachutapan, W.; Moore, R. B.; Mauritz, K. A. Asymmetric Nafion/(Zirconium Oxide) Hybrid Membranes via in Situ Sol-gel Chemistry. *J. Appl. Polym. Sci.* **1996**, *62* (2), 417–426. https://doi.org/10.1002/(sici)1097-4628(19961010)62:2<417::aid-app16>3.3.co;2-y.

(22) Noble, R. D. Perspectives on Mixed Matrix Membranes. *J. Memb. Sci.* **2011**, *378* (1–2), 393–397. https://doi.org/10.1016/j.memsci.2011.05.031.

(23) Rybak, A.; Rybak, A.; Sysel, P. Modeling of Gas Permeation through Mixed-Matrix Membranes Using Novel Computer Application MOT. *Appl. Sci.* **2018**, *8* (7), 1–20. https://doi.org/10.3390/app8071166.

(24) Anson, M.; Marchese, J.; Garis, E.; Ochoa, N.; Pagliero, C. ABS Copolymer-Activated Carbon Mixed Matrix Membranes for CO 2/CH4 Separation. *J. Memb. Sci.* **2004**, *243* (1–2), 19–28. https://doi.org/10.1016/j.memsci.2004.05.008.

(25) Yoo, Y.; Lai, Z.; Jeong, H. K. Fabrication of MOF-5 Membranes Using Microwave-Induced Rapid Seeding and Solvothermal Secondary Growth. *Microporous Mesoporous Mater.* **2009**, *123* (1–3), 100–106. https://doi.org/10.1016/j.micromeso.2009.03.036.

(26) Shah, M.; McCarthy, M. C.; Sachdeva, S.; Lee, A. K.; Jeong, H. K. Current Status of Metal-Organic Framework Membranes for Gas Separations: Promises and Challenges. *Ind. Eng. Chem. Res.* **2012**, *51* (5), 2179–2199. https://doi.org/10.1021/ie202038m.

(27) Wang, X. Y.; Zhao, F. P.; Wang, J.; Yan, Y. Bin. First-Principle Studies of Mechanical, Electronic Properties and Strain Engineering of Metal-Organic Framework. *Wuli Xuebao/Acta Phys. Sin.* **2016**, *65* (17). https://doi.org/10.7498/aps.65.178105.

(28) Aman, R.; Clearfield, A.; Sadiq, M.; Ali, Z. HKUST-1 Supported on Zirconium Phosphate as an Efficient Catalyst for Solvent Free Oxidation of Cyclohexene: DFT Study. *Catalysts* **2018**, *8* (11), 1–10. https://doi.org/10.3390/catal8110546.

(29) Davey, C. J.; Leak, D.; Patterson, D. A. Hybrid and Mixed Matrix Membranes for Separations from Fermentations. *Membranes (Basel).* **2016**, *6* (1). https://doi.org/10.3390/membranes6010017.

(30) Kolokolov, D. I.; Jobic, H.; Stepanov, A. G.; Plazanet, M.; Zbiri, M.; Ollivier, J.; Guillerm, V.; Devic, T.; Serre, C.; Férey, G. Comparison of the Dynamics of MIL-53(Cr) and MIL-47(V) Frameworks Using Neutron Scattering and DFT Methods. *Eur. Phys. J. Spec. Top.*

2010, *189* (1), 263–271. https://doi.org/10.1140/epjst/e2010-01331-y.

(31) Sabetghadam, A.; Liu, X.; Benzaqui, M.; Gkaniatsou, E.; Orsi, A.; Lozinska, M. M.; Sicard, C.; Johnson, T.; Steunou, N.; Wright, P. A.; et al. Influence of Filler Pore Structure and Polymer on the Performance of MOF-Based Mixed-Matrix Membranes for CO2 Capture. *Chem. - A Eur. J.* **2018**, *24* (31), 7949–7956. https://doi.org/10.1002/chem.201800253.

(32) Canivet, J.; Bonnefoy, J.; Daniel, C.; Legrand, A.; Coasne, B.; Farrusseng, D. Structure-Property Relationships of Water Adsorption in Metal-Organic Frameworks. *New J. Chem.* **2014**, *38* (7), 3102–3111. https://doi.org/10.1039/c4nj00076e.

(33) Meshkat, S.; Kaliaguine, S.; Rodrigue, D. Enhancing CO2 Separation Performance of Pebax® MH-1657 with Aromatic Carboxylic Acids. *Sep. Purif. Technol.* **2019**, *212* (August 2018), 901–912. https://doi.org/10.1016/j.seppur.2018.12.008.

(34) Ahmadpour, E.; Sarfaraz, M. V.; Behbahani, R. M.; Shamsabadi, A. A.; Aghajani, M. Fabrication of Mixed Matrix Membranes Containing TiO2 Nanoparticles in Pebax 1657 as a Copolymer on an Ultra-Porous PVC Support. *J. Nat. Gas Sci. Eng.* **2016**, *35*, 33–41. https://doi.org/10.1016/j.jngse.2016.08.042.

(35) Liu, Y. C.; Chen, C. Y.; Lin, G. S.; Chen, C. H.; Wu, K. C. W.; Lin, C. H.; Tung, K. L. Characterization and Molecular Simulation of Pebax-1657-Based Mixed Matrix Membranes Incorporating MoS2 Nanosheets for Carbon Dioxide Capture Enhancement. *J. Memb. Sci.* **2019**, *582* (October 2018), 358–366. https://doi.org/10.1016/j.memsci.2019.04.025.

(36) Kim, J. H.; Ha, S. Y.; Lee, Y. M. Gas Permeation of Poly(Amide-6-b-Ethylene Oxide) Copolymer. *J. Memb. Sci.* **2001**, *190* (2), 179–193. https://doi.org/10.1016/S0376-7388(01)00444-6.

(37) Han, Y.; Qi, P.; Li, S.; Feng, X.; Zhou, J.; Li, H.; Su, S.; Li, X.; Wang, B. A Novel Anode Material Derived from Organic-Coated ZIF-8 Nanocomposites with High Performance in Lithium Ion Batteries. *Chem. Commun.* **2014**, *50* (59), 8057–8060. https://doi.org/10.1039/c4cc02691h.

(38) Su, Z.; Miao, Y. R.; Zhang, G.; Miller, J. T.; Suslick, K. S. Bond Breakage under Pressure in a Metal Organic Framework. *Chem. Sci.* **2017**, *8* (12), 8004–8011. https://doi.org/10.1039/c7sc03786d.

(39) Etxeberria-Benavides, M.; David, O.; Johnson, T.; Łozińska, M. M.; Orsi, A.; Wright, P. A.; Mastel, S.; Hillenbrand, R.; Kapteijn, F.; Gascon, J. High Performance Mixed Matrix Membranes (MMMs) Composed of ZIF-94 Filler and 6FDA-DAM Polymer. *J. Memb. Sci.* **2018**, *550* (December 2017), 198–207. https://doi.org/10.1016/j.memsci.2017.12.033.

(40) https://www.ccdc.cam.ac.uk/structures/Search?Compound=ZIF8&DatabaseToSearch=Published. (Accessed on 17 June 2020).

(41) https://www.ccdc.cam.ac.uk/solutions/csd-system/components/mercury/ (Accessed on 17

June 2020).

Appendices

Appendice-1: Performance of fabricated MMMs with 6% polymer matrix in different conditions

ZIF-94 Dose (%)	***Membrane thickness (µm)***	***P CO_2 (Barrer)***	***PN_2 (Barrer)***	***Selectivity (CO_2/N_2)***	***Remarks***
0	24	43.2	1.3	32.8	PDC
2.5	29	78.3	2.2	34.9	PDC
5	41	103	2.9	34.8	PDC
10	69	96.6	2.9	33.0	PDC
15	41	107	3.1	34.4	PDC
20	55	93.5	2.7	33.7	PDC
0	14	42	35	1.2	CK
5	11	589	453	1.3	CK
10	16	570	439	1.3	CK
15	16	64.0	1.8	35.3	CK
20	16	200	118	1.7	CK
25	16	582	416	1.4	CK

Appendice-2: Permeation data of 9% matrix with different MOF dose

ZIF-94 loading (%)	***Membrane thickness (µm)***	***P CO_2 (Barrer)***	***P N_2 (Barrer)***	***Selectivity CO_2/N_2***	***Remarks***
No dose	44	2.6	0.13	20.7	*PDC*
10	**84**	**126**	**2.9**	**43.5**	***PDC***
15	42	96.6	2.9	33.1	*PDC*
20	55	105	3.3	31.3	*PDC*
25	55	2930	95.2	30.8	*PDC*

Appendice-3: Permeation data of 12% matrix with different MOF dose

ZIF-94 loading (%)	***Membrane thickness (µm)***	***P CO_2 (Barrer)***	***P N_2 (Barrer)***	***Selectivity CO_2/N_2***
No Dose	44	22.9	1.3	17.5
5	**151**	**529**	**14.1**	**37.4**
10	41	57.4	1.9	29.6
15	57	91.2	4.0	22.6